IEEE Access
Multidisciplinary | Rapid Review | Open Access Journal

Received March 6, 2019, accepted March 29, 2019, date of publication April 11, 2019, date of current version April 24, 2019.

Digital Object Identifier 10.1109/ACCESS.2019.2909783

Multiple-Toeplitz Matrices Reconstruction Algorithm for DOA Estimation of Coherent Signals

WEI ZHANG[1,2], YONG HAN[3], MING JIN[3], AND XIAOLIN QIAO[3]
[1]School of Electronics and Information Engineering, Harbin Institute of Technology, Harbin 150001, China
[2]School of Electrical & Information Engineering, North Minzu University, Yinchuan 750021, China
[3]School of Information Science and Engineering, Harbin Institute of Technology (Weihai), Weihai 264209, China

Corresponding author: Ming Jin (jmhit2013@163.com)

ABSTRACT In this paper, a new direction-of-arrival (DOA) estimation method based on multiple Toeplitz matrices reconstruction is proposed for coherent narrowband signals with a uniform linear array (ULA). First, the received signals impinging on the ULA are rearranged in a Toeplitz matrix, and a full set of correlation matrices are computed by the Toeplitz-based matrix and the observed data of each sensor. Then, a weighted summation by squaring these correlation matrices is obtained to form the full rank equivalent data covariance matrix. Furthermore, a forward-and-backward scheme is presented to improve the estimation accuracy of the covariance matrix. Based on the joint diagonalization structure of the covariance matrix with noise contributions as a scalar matrix, the angle estimation problem can be resolved by combining it with subspace-based methods. In comparison with currently known matrix reconstruction methods, the proposed algorithm applies all information contained in the correlation matrices adequately without de-noising processing in advance. Even in the case of a low signal-to-noise ratio and low snapshot number with half the array aperture reduced, the new method provides good performance on estimation and resolution. Finally, simulation results are demonstrated to verify the theoretical prediction.

INDEX TERMS Coherent signals, direction-of-arrival (DOA) estimation, Toeplitz matrix reconstruction, uniform linear array (ULA).

I. INTRODUCTION

High-resolution direction-of-arrival (DOA) estimation [1] is a major research issue in array processing [2] and has been widely used in radar [3], sonar [4], and wireless communications [5], [6]. Many subspace-based algorithms including multiple signal classification (MUSIC) [7]–[9] and estimation of signal parameters via rotational invariance techniques (ESPRIT) [10] may provide good performance for uncorrelated signals but suffer serious performance degradation when in the presence of coherent or highly correlated signal environments owing to the rank loss of the covariance matrix. An effective way to solve this problem is the spatial smoothing (SS) technique and its variants such as forward-only (FOSS) [11] and forward/backward (FBSS) spatial smoothing [12]. These methods partition the total array into several groups containing overlapping subarrays, and the average of the subarray covariance matrices with restored full rank is employed to resolve the coherent signal direction-finding combined with subspace-based algorithms. However, the subarray number is determined by the number of sources in advance, which leads to an effective decrease in aperture size and therefore a decrease in resolution capability for closely spaced arrivals.

Methods such as maximum-likelihood (ML) [13] or signal subspace fitting (SSF) [14] have been provided for resolving the coherent narrowband array problem. These methods have the advantages of not requiring eigendecomposition and not being sensitive to the coherency between impinging signals. The computation of these methods is significant because they solve complicated multidimensional iteration problems or transform multidimensional problems into sequences of one-dimensional problems through alternating maximization [15], [16].

The associate editor coordinating the review of this manuscript and approving it for publication was Yanhui Liu.

Recently, methods based on Toeplitz matrix reconstruction and its variants [17]–[24] were presented to resolve coherent signals. In [17], a data-based matrix decomposition method was used to perform the singular-value decomposition of a correlation matrix between a Toeplitz matrix constructed by the received signals and the obtained signal from an extra reference array. This makes the noise contribution a zero matrix and may combine the eigenstructure methods under a coherent signal environment. A computationally efficient algorithm named ESPRIT-like and its variants [18]–[24] has attracted the attention of researchers. In [18], the ESPRIT-like method was applied to any single row of an array output covariance matrix (AOCM). The noise effects were eliminated in advance to construct a Toeplitz matrix whose rank was only related to the DOA of the signals, and the signal subspace could be estimated by using the ESPRIT algorithm. According to the ESPRIT-like method, an improved Toeplitz matrix-based method [19] was presented to increase the dimension of the signal subspace by exploiting forward and backward vectors. Reference [20] adopted an existing ESPRIT-like scheme by exploiting half-rows of an AOCM to form a set of Toeplitz matrices in the absence of noise. The DOAs were estimated via a designed cost function that did not require a priori information of the source number. In [21]–[25], some matrix reconstruction decorrelation algorithms based on spatial differencing ideas [26] were proposed by constructing one Toeplitz matrix or several Toeplitz matrices from the covariance matrix of the received data under colored noise field. The maximum number of resolvable sources could potentially exceed the number of sensors. However, in most of these spatial differencing based methods, the DOAs of uncorrelated and coherent signals are estimated separately, which increased the computational burden. Moreover, their performance may become poor under a relatively small snapshot in the case of the non-zero residual correlations between the presupposed structural properties to be invalid.

Many other matrix reconstruction algorithms which were based on higher-order cumulants [27] have also been developed for coherent signal DOA estimation in order to resolve more signals in the presence of color Gaussian noise fields. Reference [28] presented a fourth-order cumulants-based Toeplitz matrices reconstruction (FOC-TMR) method by arranging the cumulants elements of received signals from two parallel uniform linear arrays (ULAs) to two Toeplitz matrices. An effective decoherence method introduced in [29] extended the ESPRIT-like algorithm to achieve the DOA estimation of incident narrowband coherent signals by applying half-rows of an AOCM to reconstruct a set of fourth-order cumulants-based Toeplitz matrices. In [30], an improved FOC-TMR algorithm was addressed to reconstruct two matrices by utilizing two parallel ULAs and the changing reference array element. Unfortunately, such methods require large numbers of snapshots and suffer from burdensome computation. In addition, the data matrix construction methods were also extended in many other applications such as two-dimensional (2D) DOA estimation [31]–[33] and multiple-input multiple-output (MIMO) radar [34]–[36].

As mentioned above, there are two major problems among the existing Toeplitz matrix reconstruction methods. First, although they may be applicable by directly combining with subspace-based methods by applying auxiliary arrays or the central row of the AOCM to obtain a date-based Toeplitz covariance matrix (which allows the noise term to be a zero matrix or scalar matrix), adding an auxiliary array may increase costs and reduce the effective array aperture.

Second, when employing one noncentral row or partial rows of the AOCM for Toeplitz matrix construction, the noise contribution of the resulting matrix cannot be a scalar matrix. Therefore, DOA estimates should be obtained after the noise contribution is eliminated, which increases the computational burden. Furthermore, simply applying one row or partial rows of the covariance matrix could result in incomplete information utilization of the AOCM as well as a degradation in the resolving capability in terms of the estimation accuracy.

In this paper, we propose a new algorithm to overcome the aforementioned shortcomings of the existing methods. The proposed algorithm can employ the complete information of all array outputs to reconstruct the full set of Toeplitz matrices and produce better estimates of the covariance matrix. Unlike other Toeplitz matrix reconstruction methods, the proposed approach does not require auxiliary array or noise elimination.

This paper is organized as follows. We present the data model in Section II and derive our algorithm in Section III. Section IV provides numerical examples. Finally, we give our conclusions in Section V.

Notation: Matrices, vectors and scalar quantities are denoted by uppercase boldface, lowercase boldface, and lowercase letters, respectively. Superscripts $(\cdot)^H$, $(\cdot)^T$ and $(\cdot)^*$ represent a conjugate transpose, transpose and conjugate, respectively. The operator $\mathrm{E}[\cdot]$ is the expectation. $\mathbf{0}_{m\times n}$, $\boldsymbol{I}_m$ and diag $(\cdot)$ denote the $m \times n$ zero matrix, $m \times m$ identity matrix, and the diagonal matrix, respectively.

II. PROBLEM FORMULATION

Consider a ULA with $2M + 1$ isotropic sensors as shown in Fig. 1. Suppose there are $P\,(P < M + 1)$ narrowband far-field sources impinging on the array from distinct directions $\theta_p, p = 1, 2, \ldots, P$. Let the index of the central array element be 0. $d = \lambda/2$ is the spacing between the adjacent sensors, and λ is the carrier wavelength.

For the sake of notational simplicity, we define the $(2M + 1) \times 1$ array output vector at time t in the noiseless case as

$$\begin{aligned}\boldsymbol{x}(t) &= [x_{-M}(t), \ldots, x_0(t), \ldots, x_M(t)]^T \\ &= \boldsymbol{A}\boldsymbol{s}(t) = \sum_{p=1}^{P} \boldsymbol{a}(\theta_p)\, s_p(t). \end{aligned} \tag{1}$$

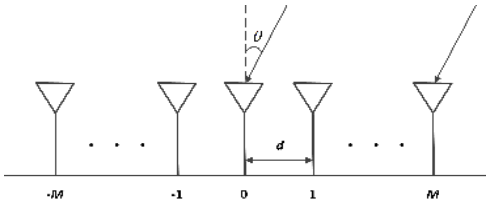

FIGURE 1. Antenna array model.

Then, in the presence of noise, the $(2M+1)\times 1$ array output vector at time t is given as

$$\begin{aligned}\boldsymbol{y}(t) &= [y_{-M}(t),\ldots,y_0(t),\ldots,y_M(t)]^T \\ &= \boldsymbol{x}(t)+\boldsymbol{n}(t)=\boldsymbol{A}\boldsymbol{s}(t)+\boldsymbol{n}(t).\end{aligned} \tag{2}$$

where $\boldsymbol{s}(t)=[s_1(t),\ldots,s_P(t)]^T$ denotes the $P\times 1$ source signal vector, where the P signals can be uncorrelated, partially correlated, or coherent. $\boldsymbol{A}=[\boldsymbol{a}(\theta_1),\ldots,\boldsymbol{a}(\theta_P)]$ is the $(2M+1)\times P$ array steering matrix with $\boldsymbol{a}(\theta_p)=\left[e^{-j(2\pi/\lambda)Md\sin\theta_p},\ldots,1,\ldots,e^{j(2\pi/\lambda)Md\sin\theta_p}\right]^T$ as the pth $(2M+1)\times 1$ steering vector. $\boldsymbol{n}(t)=[n_{-M}(t),\ldots,n_0(t),\ldots,n_M(t)]^T$ is the $(2M+1)\times 1$ Gaussian white-noise vector assumed to be uncorrelated to signals with zero mean and variance σ_n^2.

III. PROPOSED ALGORITHM

First, we construct an $(M+1)\times(M+1)$ Toeplitz matrix via $\boldsymbol{x}(t)$ as follows:

$$\boldsymbol{R}_X(t)=\begin{bmatrix} x_0(t) & x_1(t) & \cdots & x_M(t) \\ x_{-1}(t) & x_0(t) & \cdots & x_{M-1}(t) \\ \vdots & \vdots & \ddots & \vdots \\ x_{-M}(t) & x_{-M+1}(t) & \cdots & x_0(t)\end{bmatrix} \tag{3}$$

Let $\boldsymbol{S}(t)=\mathrm{diag}\{s_1(t),\ldots,s_P(t)\}$. Then, (3) can be rewritten as

$$\boldsymbol{R}_X(t)=\tilde{\boldsymbol{A}}\boldsymbol{S}(t)\tilde{\boldsymbol{A}}^H. \tag{4}$$

Here, $\tilde{\boldsymbol{A}}=[\tilde{\boldsymbol{a}}(\theta_1),\ldots,\tilde{\boldsymbol{a}}(\theta_P)]$ is the $(M+1)\times P$ array steering matrix with $\tilde{\boldsymbol{a}}(\theta_p)=[1,e^{-j(2\pi/\lambda)d\sin\theta_p},\ldots,e^{-j(2\pi/\lambda)Md\sin\theta_p}]^T$. The correlation between $\boldsymbol{R}_X(t)$ and obtained signal $x_i(t)$ from the ith array $(i=-M,\ldots,0,\ldots,M)$ is given by

$$\boldsymbol{R}_{Xi}=\mathrm{E}\left[\boldsymbol{R}_X(t)x_i^*(t)\right]=\tilde{\boldsymbol{A}}\mathrm{E}\left[\boldsymbol{S}(t)x_i^*(t)\right]\tilde{\boldsymbol{A}}^H=\tilde{\boldsymbol{A}}\tilde{\boldsymbol{S}}_i\tilde{\boldsymbol{A}}^H \tag{5}$$

where $\tilde{\boldsymbol{S}}_i=\mathrm{E}\left[\boldsymbol{S}(t)x_i^*(t)\right]$ represents the correlation matrix between $\boldsymbol{S}(t)$ and $x_i(t)$.

Similar to (3), a $(M+1)\times(M+1)$ Toeplitz data matrix formed by $\boldsymbol{y}(t)$ has the following expression:

$$\begin{aligned}\boldsymbol{R}_Y(t) &= \begin{bmatrix} y_0(t) & y_1(t) & \cdots & y_M(t) \\ y_{-1}(t) & y_0(t) & \cdots & y_{M-1}(t) \\ \vdots & \vdots & \ddots & \vdots \\ y_{-M}(t) & y_{-M+1}(t) & \cdots & y_0(t)\end{bmatrix} \\ &= \boldsymbol{R}_X(t)+\boldsymbol{R}_N(t).\end{aligned} \tag{6}$$

where $\boldsymbol{R}_N(t)=\begin{bmatrix} n_0(t) & n_1(t) & \cdots & n_M(t) \\ n_{-1}(t) & n_0(t) & \cdots & n_{M-1}(t) \\ \vdots & \vdots & \ddots & \vdots \\ n_{-M}(t) & n_{-M+1}(t) & \cdots & n_0(t)\end{bmatrix}$ is the $(M+1)\times(M+1)$ Toeplitz matrix constructed by the noise vector $\boldsymbol{n}(t)$.

In a similar way, the $(M+1)\times(M+1)$ correlation matrix between $\boldsymbol{R}_Y(t)$ and the ith element output $y_i(t)$ is written as

$$\begin{aligned}\boldsymbol{R}_{Yi} &= \mathrm{E}\left[\boldsymbol{R}_Y(t)y_i^*(t)\right] \\ &= \mathrm{E}\left[\boldsymbol{R}_X(t)x_i^*(t)\right]+\mathrm{E}\left[\boldsymbol{R}_N(t)n_i^*(t)\right] \\ &= \boldsymbol{R}_{Xi}+\sigma_n^2\tilde{\boldsymbol{I}}_{(M+1),i}.\end{aligned} \tag{7}$$

where $\tilde{\boldsymbol{I}}_{(M+1),i}$ is an $(M+1)\times(M+1)$ matrix with all zeros except for the unity elements on the ith diagonal, and $\tilde{\boldsymbol{I}}_{(M+1),0}$ equals the $(M+1)\times(M+1)$ identity matrix $\boldsymbol{I}_{M+1}$ with $i=0$, in particular.

From (7), we observe that the correlation matrix $\boldsymbol{R}_{Yi}$ that is obtained between $\boldsymbol{R}_Y(t)$ and the received signal from ith array $y_i(t)$ is equivalent to employing the ith row of the AOCM $\boldsymbol{R}_Y$=E$\left[\boldsymbol{y}(t)\boldsymbol{y}^H(t)\right]$ for constructing a Toeplitz matrix, similar to the ESPRIT-like method in [18]. Obviously, utilizing the central array $(i=0)$ output $y_i(t)$ and $\boldsymbol{R}_Y(t)$ to obtain $\boldsymbol{R}_{Yi}, \tilde{\boldsymbol{I}}_{(M+1),0}$ of (7) results in an identity matrix, which allows us to perform eigenvalue decomposition directly for acquiring the solution of the signal subspace.

When selecting the noncentral array $(i\neq 0)$ element to obtain $\boldsymbol{R}_{Yi}$, the noise components from $\sigma_n^2\tilde{\boldsymbol{I}}_{(M+1),i}$ are uniformly distributed along the diagonal line parallel to the main diagonal line of the noise matrix. This means the noise term cannot become a scalar matrix, and the signal subspace cannot be obtained by directly carrying out the eigenstructure methods from $\boldsymbol{R}_{Yi}$ for the DOA estimate.

To avoid only utilizing the partial information of the AOCM and depressing the noise process, which may lead to degradation of the DOA estimation performance, a new reconstructed Toeplitz matrix method is proposed by exploiting the overall signal and noise information of $\boldsymbol{R}_{Yi}$ from $i\in[-M,M]$. The DOA estimation can be realized by obtaining the diagonalization structure of the noise term without requiring denoising processing in advance.

Given $\tilde{\boldsymbol{R}}$ by the sum of squaring $\boldsymbol{R}_{Yi}$ respectively from $i\in[-M,M]$,

$$\begin{aligned}\tilde{\boldsymbol{R}} &= \sum_{i=-M}^{M}\boldsymbol{R}_{Yi}\boldsymbol{R}_{Yi}^H \\ &= \sum_{i=-M}^{M}\left[\left(\boldsymbol{R}_{Xi}+\sigma_n^2\tilde{\boldsymbol{I}}_{(M+1),i}\right)\left(\boldsymbol{R}_{Xi}+\sigma_n^2\tilde{\boldsymbol{I}}_{(M+1),i}\right)^H\right] \\ &= \sum_{i=-M}^{M}\boldsymbol{R}_{Xi}\boldsymbol{R}_{Xi}^H+\sum_{i=-M}^{M}\boldsymbol{R}_{Xi}\sigma_n^2\tilde{\boldsymbol{I}}_{(M+1),i}^H \\ &\quad+\sum_{i=-M}^{M}\sigma_n^2\tilde{\boldsymbol{I}}_{(M+1),i}\boldsymbol{R}_{Xi}^H+\sum_{i=-M}^{M}\sigma_n^4\tilde{\boldsymbol{I}}_{(M+1),i}\tilde{\boldsymbol{I}}_{(M+1),i}^H.\end{aligned} \tag{8}$$

Considering the first term of (8), inserting (5) into the first term of (8) gives

$$\sum_{i=-M}^{M} \boldsymbol{R}_{Xi}\boldsymbol{R}_{Xi}^{H} = \tilde{\boldsymbol{A}} \sum_{i=-M}^{M} \tilde{\boldsymbol{S}}_i \tilde{\boldsymbol{A}}^{H} \tilde{\boldsymbol{A}} \tilde{\boldsymbol{S}}_i^{H} \tilde{\boldsymbol{A}}^{H}. \tag{9}$$

For the second term of (8) (see Appendix A for details), we can write that

$$\sum_{i=-M}^{M} \boldsymbol{R}_{Xi}\sigma_n^2 \tilde{\boldsymbol{I}}_{(M+1),i}^{H} = \sigma_n^2 \tilde{\boldsymbol{A}} \sum_{k=0}^{M} \boldsymbol{D}^k \boldsymbol{R}_S \left(\boldsymbol{D}^k\right)^{H} \tilde{\boldsymbol{A}}^{H}. \tag{10}$$

where $\boldsymbol{R}_S = \mathrm{E}\left[\boldsymbol{s}(t)\,\boldsymbol{s}^{H}(t)\right]$ denotes the source covariance matrix, and $\boldsymbol{D} = \mathrm{diag}\left\{e^{j(2\pi/\lambda)d\sin\theta_1}, \ldots, e^{j(2\pi/\lambda)d\sin\theta_P}\right\}$.

In a similar way, the third term of (8) can be computed as follows (see Appendix A):

$$\sum_{i=-M}^{M} \sigma_n^2 \tilde{\boldsymbol{I}}_{(M+1),i} \boldsymbol{R}_{Xi}^{H} = \sigma_n^2 \tilde{\boldsymbol{A}} \sum_{k=0}^{M} \boldsymbol{D}^k \boldsymbol{R}_s \left(\boldsymbol{D}^k\right)^{H} \tilde{\boldsymbol{A}}^{H}. \tag{11}$$

From (10) and (11), we find that only summing all of the individual signals and noise cross-terms of $\boldsymbol{R}_{Xi}\sigma_n^2\tilde{\boldsymbol{I}}_{(M+1),i}^{H}$ or $\sigma_n^2\tilde{\boldsymbol{I}}_{(M+1),i}\boldsymbol{R}_{Xi}^{H}$ can construct the equivalent source covariance matrix.

Considering the fourth term of (8), $\tilde{\boldsymbol{I}}_{(M+1),i}\tilde{\boldsymbol{I}}_{(M+1),i}^{H}$ can be written as

$$\tilde{\boldsymbol{I}}_{(M+1),i}\tilde{\boldsymbol{I}}_{(M+1),i}^{H} = \begin{cases} \begin{bmatrix} \boldsymbol{I}_{(M+1-i)\times(M+1-i)} & \boldsymbol{0}_{(M+1-i)\times i} \\ \boldsymbol{0}_{i\times(M+1-i)} & \boldsymbol{0}_{i\times i} \end{bmatrix}, & i \geq 0 \\ \begin{bmatrix} \boldsymbol{0}_{(-i)\times(-i)} & \boldsymbol{0}_{(-i)\times(M+1+i)} \\ \boldsymbol{0}_{(M+1+i)\times(-i)} & \boldsymbol{I}_{(M+1+i)\times(M+1+i)} \end{bmatrix}, & i < 0 \end{cases} \tag{12}$$

Substituting (12) in the fourth term of (8), we have

$$\sum_{i=-M}^{M} \sigma_n^4 \tilde{\boldsymbol{I}}_{(M+1),i}\tilde{\boldsymbol{I}}_{(M+1),i}^{H} = (M+1)\,\sigma_n^4 \tilde{\boldsymbol{I}}_{(M+1),0}. \tag{13}$$

According to the result from (13), applying only half-rows of the AOCM to construct a set of Toeplitz matrices (equivalently summing the products of $\boldsymbol{R}_{Yi}$ and $\boldsymbol{R}_{Yi}^{H}$ from $i \in [-M, 0]$) results in a noise contribution that is not a scalar matrix. Thus, the estimates of the equivalent covariance matrix can be available if the noise effect is neglected or eliminated. Our method can acquire a scalar matrix just by summing all of the terms corresponding to the noise contribution.

By combining (9)–(13), (8) can be simplified as

$$\tilde{\boldsymbol{R}} = \tilde{\boldsymbol{A}} \left(\sum_{i=-M}^{M} \tilde{\boldsymbol{S}}_i \tilde{\boldsymbol{A}}^{H} \tilde{\boldsymbol{A}} \tilde{\boldsymbol{S}}_i^{H} + 2\sigma_n^2 \sum_{k=0}^{M} \boldsymbol{D}^k \boldsymbol{R}_S \left(\boldsymbol{D}^k\right)^{H} \right) \tilde{\boldsymbol{A}}^{H} + (M+1)\,\sigma_n^4 \tilde{\boldsymbol{I}}_{(M+1),0} \tag{14}$$

Here, we define

$$\tilde{\boldsymbol{R}}_S = \sum_{i=-M}^{M} \tilde{\boldsymbol{S}}_i \tilde{\boldsymbol{A}}^{H} \tilde{\boldsymbol{A}} \tilde{\boldsymbol{S}}_i^{H} + 2\sigma_n^2 \sum_{k=0}^{M} \boldsymbol{D}^k \boldsymbol{R}_S \left(\boldsymbol{D}^k\right)^{H} \tag{15}$$

and $\tilde{\boldsymbol{R}}$ can be rewritten as follows:

$$\tilde{\boldsymbol{R}} = \tilde{\boldsymbol{A}} \tilde{\boldsymbol{R}}_S \tilde{\boldsymbol{A}}^{H} + (M+1)\,\sigma_n^4 \tilde{\boldsymbol{I}}_{(M+1),0} \tag{16}$$

It is shown in (15) that since $\sum_{i=-M}^{M} \tilde{\boldsymbol{S}}_i \tilde{\boldsymbol{A}}^{H} \tilde{\boldsymbol{A}} \tilde{\boldsymbol{S}}_i^{H}$ can be expressed as $\sum_{k=0}^{M} \boldsymbol{D}^k \left(\sum_{i=-M}^{M} \boldsymbol{R'}_S \right) \left(\boldsymbol{D}^k\right)^{H}$ (see Appendix B), the $\sum_{i=-M}^{M} \tilde{\boldsymbol{S}}_i \tilde{\boldsymbol{A}}^{H} \tilde{\boldsymbol{A}} \tilde{\boldsymbol{S}}_i^{H}$ and $2\sigma_n^2 \sum_{k=0}^{M} \boldsymbol{D}^k \boldsymbol{R}_S \left(\boldsymbol{D}^k\right)^{H}$ terms of $\tilde{\boldsymbol{R}}_S$ are essentially equal to the $(M+1)$ -order equivalent source covariance matrix of the FOSS algorithm [11]. Hence, $\tilde{\boldsymbol{R}}_S$ is a positive definite matrix with a full rank P. Furthermore, the rank P of our method is only related to the DOAs of signals and is independent of the coherence of the incident signals by the assumption made by the sources in Section II.

To improve the estimation performance, we consider facilitating (16) by the forward/backward smoothing technique as

$$\boldsymbol{R}_M = \tilde{\boldsymbol{R}} + \boldsymbol{J}\tilde{\boldsymbol{R}}^{*}\boldsymbol{J} \tag{17}$$

where $\boldsymbol{J}$ denotes the $(M+1) \times (M+1)$ exchange matrix with ones on its antidiagonal and zeros elsewhere. According to (17), $\boldsymbol{R}_M$ is obtained with the noise term a scalar matrix as well, which allows us to find the column space of $\tilde{\boldsymbol{A}}$ only by eigendecomposing $\boldsymbol{R}_M$ without eliminating the noise contribution in advance.

In addition, note that $\tilde{\boldsymbol{R}}_S$ in (15) has an extra equivalent source covariance matrix $\sum_{i=-M}^{M} \tilde{\boldsymbol{S}}_i \tilde{\boldsymbol{A}}^{H} \tilde{\boldsymbol{A}} \tilde{\boldsymbol{S}}_i^{H}$ when compared to the FOSS algorithm. Similarly, after forward/backward averaging, the equivalent source covariance matrix of the MTOEP-root has one more term than the FBSS algorithm [12], which indicates that our algorithm exploits the overall information of the $(2M+1)$ -order data covariance matrix to reconstruct the $(M+1)$ -order equivalent source covariance matrix. However, FBSS-root or FOSS-root use the principal diagonal autocorrelation information of the data covariance matrix to form the smoothed source covariance matrix, whose order depends on the smoothing number. Finally, the root-MUSIC method [37] without a space spectrum search can be applied to obtain the DOAs of the sources.

Detailed steps for implementing our proposed algorithm, which is called MTOEP-root, are listed in Table 1.

IV. SIMULATION RESULTS

In this section, we present numerical examples to evaluate the performance of our proposed MTOEP-root method as compared with the FOSS, FBSS, and ESPRIT-like methods in terms of the root-mean-square error (RMSE) and probability of resolution. To be fair, the root-MUSIC algorithm is also applied to find the DOAs for the FOSS and FBSS schemes. The Cramér-Rao bound (CRB) given in [38] is applied for comparison reference in the former.

We assume that all narrowband sources are of equal power with a center frequency of 9 MHz, and the sampling

TABLE 1. Pseudocode of MTOEP-root algorithm.

Step 1: Record N snapshots of array output vector $\mathbf{y}(t)$. Each of them forms the Toeplitz matrix as (6) to obtain $\boldsymbol{R}_{y}(t)$;

Step 2: Apply $\boldsymbol{R}_{yi} = \frac{1}{N}\sum_{t=1}^{N} \boldsymbol{R}_{y}(t)\, y_i^{*}(t)$ instead of (7) to calculate the correlation matrix between $\boldsymbol{R}_{y}(t)$ and $y_i(t)$;

Step 3: Select the overall $\boldsymbol{R}_{yi}$ from $i \in [-M, M]$. Let $\tilde{\boldsymbol{R}} = \sum_{i=-M}^{M} \hat{\boldsymbol{R}}_{yi}\hat{\boldsymbol{R}}_{yi}^{H}$ instead of (8) to obtain $\tilde{\boldsymbol{R}}$;

Step 4: Utilize $\boldsymbol{R}_{M} = \tilde{\boldsymbol{R}} + \boldsymbol{J}\tilde{\boldsymbol{R}}^{*}\boldsymbol{J}$ instead of (17) to obtain $\boldsymbol{R}_{M}$;

Step 5: Exploit root method to estimate the real DOAs.

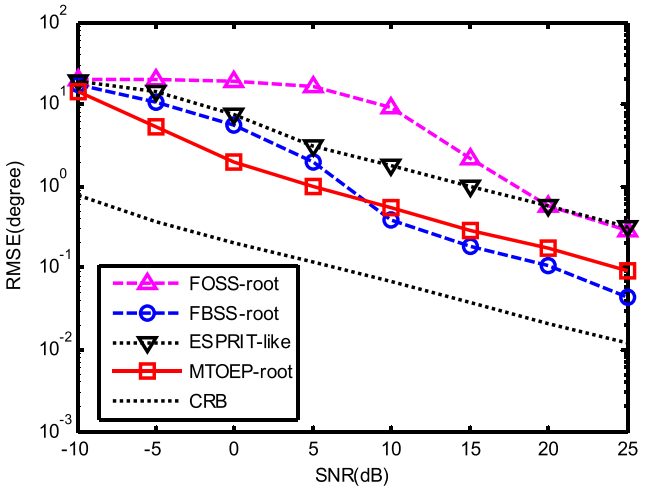

FIGURE 2. RMSE vs. SNR for one uncorrelated signal and three coherent signals with DOAs of 53°, −2°, 8°, 22°. The number of snapshots is 200.

frequency is set to 1000 Hz. The input signal-to-noise ratio (SNR) of the pth source is defined as SNR $= 10\log_{10}\left(\sigma_p^2 \big/ \sigma_n^2\right)$, and the RMSE of the DOA estimates is defined as $\text{RMSE}_\theta = \sqrt{\frac{1}{WP}\sum_{i=1}^{P}\sum_{w=1}^{W}(\hat{\theta}_{i,w} - \theta_i)^2}$, where W is the number of Monte Carlo runs, and P is the number of all sources. Consider $\left|\hat{\theta}_{i,w} - \theta_i\right|$ less than 1° as a successful resolution. A total of 1000 Monte Carlo trails are performed to obtain the statistic results in our examples, and there is a random phase delay from $[0, 2\pi]$ between these signals at each Monte Carlo trail.

In the first example, the RMSE and probability of resolution performance as a function of the SNR are examined. We consider four sources: one uncorrelated signal from 53° and a group of three coherent signals from (−2°, 8°, 22°) with a nine-element half-wavelength ULA, that is, $M = 4$. The number of snapshots taken is 200, and the number of subarrays for FOSS and FBSS are 4 and 3, respectively.

From the simulation results shown in Fig. 2, when coherent and uncorrelated sources exist, it can be clearly seen that

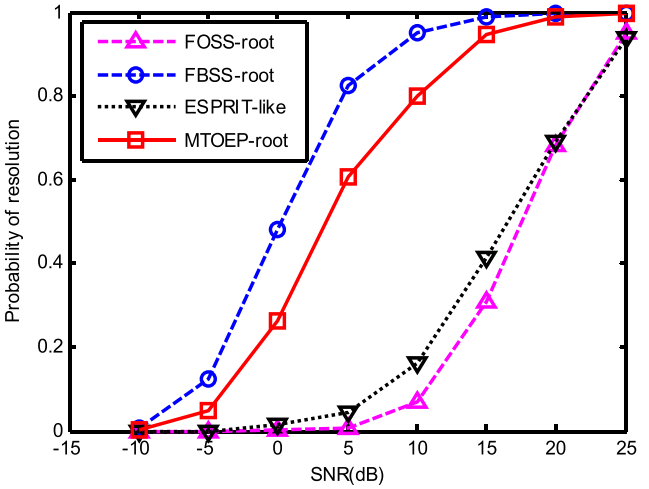

FIGURE 3. Probability of resolution vs. SNR for one uncorrelated signal and three coherent signals with DOAs of 53°, −2°, 8°, 22°. The number of snapshots is 200.

our proposed MTOEP-root achieves a much better RMSE performance than the FOSS-root and ESPRIT-like methods over the entire SNR region. Meanwhile, our proposed method can produce better RMSEs than the FBSS-root algorithm in the low-SNR regime and is slightly inferior at high SNRs.

Fig. 3 shows that our proposed MTOEP-root method has lower-resolution DOA estimation than the FBSS-root method, and obviously outperforms the FOSS-root and ESPRIT-like methods at any SNR. In particular, when the SNR is 15 dB, the resolution probability in our scheme and FBSS-root are above 90%, while those of the other two estimators are below 50%.

In the second example, we investigate the RMSE and probability of resolution vs. the number of snapshots. The simulation conditions are similar to those in example 1, except that the number of snapshots varies from 10 to 800 and the SNR is fixed at 20 dB.

It can be seen in Fig. 4 that our MTOEP-root achieves better performance than the FBSS-root scheme for a considerably low number of snapshots such as 10, and a little less when increasing the number of snapshots. In the entire snapshot regime, our MTOEP-root method produces much better RMSEs than the FOSS-root and ESPRIT-like methods. Fig. 5 also illustrates that the resolution probability of our MTOEP-root and FBSS-root methods is much higher than those of the other two estimators, especially for a low number of snapshots.

In the third example, we test the estimation performance in terms of the angular separation between two coherent signals. One signal comes from 5°, and the other signal is $5° + \Delta\theta$ with the angular separation $\Delta\theta$ varied from 2° to 22°. The SNR is 5 dB, while the number of snapshots is fixed at 32. The number of subarrays for FOSS and FBSS are 2 and 1, respectively.

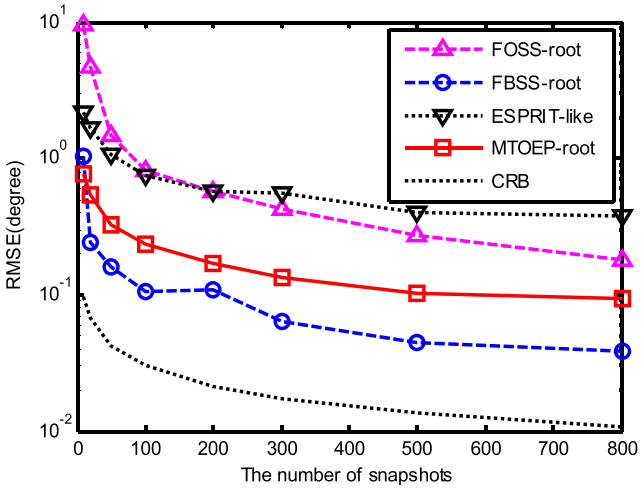

FIGURE 4. RMSE vs. number of snapshots for one uncorrelated signal and three coherent signals with DOAs of 53°, −2°, 8°, 22°. SNR is 20 dB.

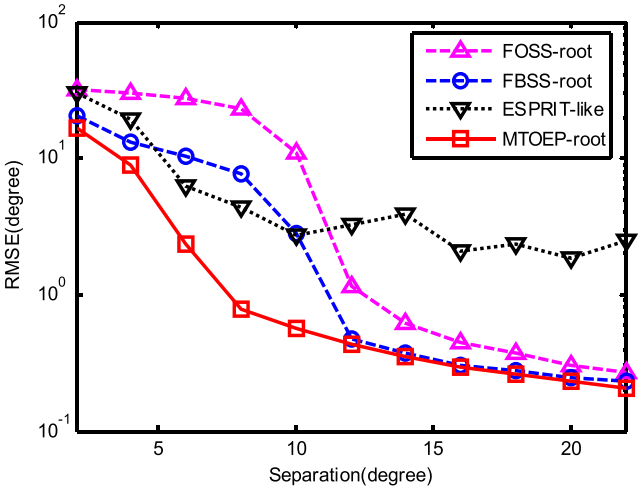

FIGURE 6. RMSE vs. angular separation for two coherent signals with DOAs of 5°, 5° + $\Delta\theta$. SNR is 5 dB and the number of snapshots is 32.

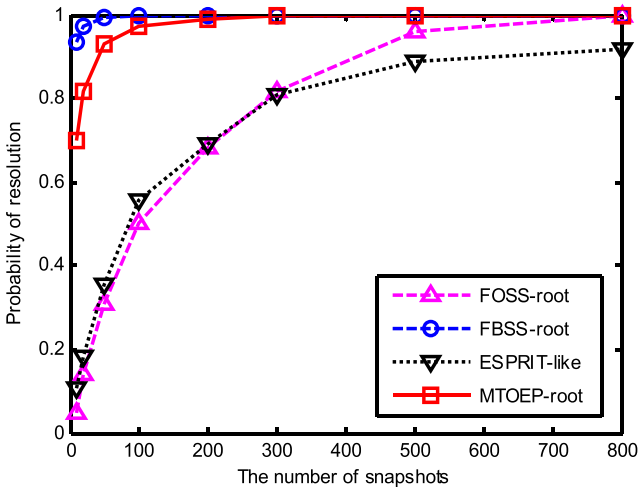

FIGURE 5. Probability of resolution vs. number of snapshots for one uncorrelated signal and three coherent signals with DOAs of 53°, −2°, 8°, 22°. SNR is 20 dB.

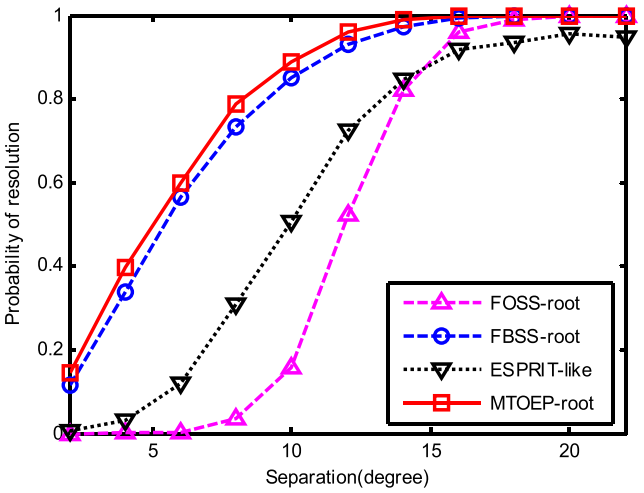

FIGURE 7. Probability of resolution vs. angular separation for two coherent signals with DOAs of 5°, 5° + $\Delta\theta$. SNR is 5 dB and the number of snapshots is 32.

We can see in Fig. 6 that with an increase in the angular separation, our MTOEP-root method has much better RMSEs than the other three algorithms in the case of low SNR and few samples, especially when the DOAs between the coherent sources are relatively close. When the angular separation between the two coherent sources is enlarged, the RMSE curves of the FBSS-root method gradually approach those of our method. Fig. 7 shows that the probability of resolution of our MTOEP-root method is slightly higher than that of FBSS-root, and is clearly higher than the ESPRIT-like and FOSS-root methods across the entire angular separation regime.

The simulation results from Fig. 2 to Fig. 5 show that ESPRIT-like used only one row of the data covariance matrix and FBSS-root and FOSS-root use the principal diagonal autocorrelation information of the data covariance matrix. However, our MTOEP-root adequately uses all correlation information of the data covariance matrix, and therefore has the best estimation accuracy and resolution probability in the low/middle SNRs and few number of snapshots.

Because of the limitation of the aperture of the array, our method can estimate M sources with at least $2M + 1$ sensors, which means that half the array aperture is lost as in the ESPRIT-like method. The array aperture of FBSS is larger than that of our algorithm. When the number of mixed coherent and uncorrelated signals is high with an increase in snapshot numbers and high SNRs, FBSS has better resolution and estimation performance than our method.

From Fig. 6 and Fig. 7, we show that when the number of coherent sources to be resolved is small and the coherent source angles are close, our algorithm has better estimation accuracy and resolution probability. The information utilization in our method is the best among the three methods, especially under a low SNR and small snapshot.

V. CONCLUSIONS

A new direction-finding algorithm called MTOEP-root was proposed for coherent signals. First, we constructed a data-based Toeplitz matrix directly from all arrays of received data. Based on this Toeplitz matrix, a set of the correlation matrices between it and the received data from each array was computed. Then, the new data matrix was calculated by summing the products of these correlation matrices and their associated matrices. Finally, after exploiting forward/backward averaging, we obtained the equivalent full rank covariance matrix for decorrelating the source signals with the noise term as a scalar matrix.

As compared with existing subspace-based decorrelation estimators, the most significant advantage of the our proposed estimator is that it can apply all correlation information of the received data from the overall array sensors. In addition, the coherent signals are resolved with a reconstructed Toeplitz matrix without requiring elimination of the noise contribution in advance. The numerical results demonstrated the effectiveness of the proposed algorithm.

APPENDIX A

In this appendix, we prove that (10) and (11) hold.

Substituting (5) into the second term of (8), we have

$$\begin{aligned}\sum_{i=-M}^{M}\boldsymbol{R}_{Xi}\sigma_n^2\tilde{\boldsymbol{I}}_{(M+1),i}^H &= \sigma_n^2\sum_{i=-M}^{M}\mathrm{E}\left[\boldsymbol{R}_X(t)\,x_i^*(t)\,\boldsymbol{I}_{(M+1),i}^H\right]\\ &= \sigma_n^2\mathrm{E}\left[\boldsymbol{R}_X(t)\sum_{i=-M}^{M}x_i^*(t)\,\boldsymbol{I}_{(M+1),i}^H\right]\\ &= \sigma_n^2\mathrm{E}\left[\boldsymbol{R}_X(t)\,\boldsymbol{R}_X^H(t)\right]. \end{aligned}\tag{18}$$

Inserting (4) into (18), we obtain

$$\sigma_n^2\mathrm{E}\left[\boldsymbol{R}_X(t)\,\boldsymbol{R}_X^H(t)\right]=\sigma_n^2\tilde{\boldsymbol{A}}\mathrm{E}\left[\boldsymbol{S}(t)\,\tilde{\boldsymbol{A}}^H\tilde{\boldsymbol{A}}\boldsymbol{S}^H(t)\right]\tilde{\boldsymbol{A}}^H.\tag{19}$$

We define

$$\tilde{\boldsymbol{A}}^H=[\boldsymbol{b}_0,\ldots,\boldsymbol{b}_k,\ldots,\boldsymbol{b}_M].\tag{20}$$

with $\boldsymbol{b}_k = \left[e^{j2\pi kd\sin\theta_1/\lambda}, e^{j2\pi kd\sin\theta_2/\lambda},\ldots,e^{j2\pi kd\sin\theta_P/\lambda}\right]$, $(k=0,1,\ldots,M)$. Then, we have

$$\begin{aligned}\mathrm{E}\left[\boldsymbol{S}(t)\,\tilde{\boldsymbol{A}}^H\tilde{\boldsymbol{A}}\boldsymbol{S}^H(t)\right] &= \mathrm{E}\left[\boldsymbol{S}(t)\sum_{k=0}^{M}\boldsymbol{b}_k\boldsymbol{b}_k^H\boldsymbol{S}^H(t)\right]\\ &= \sum_{k=0}^{M}\mathrm{E}\left\{[\boldsymbol{S}(t)\,\boldsymbol{b}_k]\,[\boldsymbol{S}(t)\,\boldsymbol{b}_k]^H\right\}.\end{aligned}\tag{21}$$

Let $\boldsymbol{D}=\mathrm{diag}(\boldsymbol{b}_1)$. Then, $\boldsymbol{D}^k=\mathrm{diag}(\boldsymbol{b}_k)$. Since $\boldsymbol{S}(t)\,\boldsymbol{b}_k = \mathrm{diag}\{s_1(t),\ldots,s_P(t)\}\,\boldsymbol{b}_k = \mathrm{diag}(\boldsymbol{b}_k)\,\boldsymbol{s}(t)$, (21) can be expressed as

$$\mathrm{E}\left[\boldsymbol{S}(t)\,\tilde{\boldsymbol{A}}^H\tilde{\boldsymbol{A}}\boldsymbol{S}^H(t)\right]=\sum_{k=0}^{M}\boldsymbol{D}^k\boldsymbol{R}_S\left(\boldsymbol{D}^k\right)^H.\tag{22}$$

where $\boldsymbol{R}_S = \mathrm{E}\left[\boldsymbol{s}(t)\,\boldsymbol{s}^H(t)\right]$ is the $P\times P$ signal covariance matrix.

Consequently, from (19)–(22), we determine (18) as follows:

$$\sum_{i=-M}^{M}\boldsymbol{R}_{Xi}\sigma_n^2\boldsymbol{I}_{(M+1),i}^H=\sigma_n^2\tilde{\boldsymbol{A}}\sum_{k=0}^{M}\boldsymbol{D}^k\boldsymbol{R}_S\left(\boldsymbol{D}^k\right)^H\tilde{\boldsymbol{A}}^H.$$

holds.

Similarly, substituting (5) into the third term of (8) and combining the results of (19)–(22), we obtain

$$\sum_{i=-M}^{M}\sigma_n^2\boldsymbol{I}_{(M+1),i}\boldsymbol{R}_{Xi}^H=\sigma_n^2\tilde{\boldsymbol{A}}\sum_{k=0}^{M}\boldsymbol{D}^k\boldsymbol{R}_s\left(\boldsymbol{D}^k\right)^H\tilde{\boldsymbol{A}}^H.$$

holds.

Consequently, (10) and (11) hold.

APPENDIX B

In this appendix, we prove that $\sum_{i=-M}^{M}\tilde{\boldsymbol{S}}_i\tilde{\boldsymbol{A}}^H\tilde{A}\tilde{\boldsymbol{S}}_i^H$ in (15) can be expressed as $\sum_{k=0}^{M}\boldsymbol{D}^k\left(\sum_{i=-M}^{M}\boldsymbol{R'}_S\right)\left(\boldsymbol{D}^k\right)^H$.

Substituting (20) into $\tilde{\boldsymbol{S}}_i\tilde{\boldsymbol{A}}^H\tilde{\boldsymbol{A}}\tilde{\boldsymbol{S}}_i^H$, we have

$$\tilde{\boldsymbol{S}}_i\tilde{\boldsymbol{A}}^H\tilde{\boldsymbol{A}}\tilde{\boldsymbol{S}}_i^H=\tilde{\boldsymbol{S}}_i\sum_{k=0}^{M}\boldsymbol{b}_k\boldsymbol{b}_k^H\tilde{\boldsymbol{S}}_i^H=\sum_{k=0}^{M}\left(\tilde{\boldsymbol{S}}_i\boldsymbol{b}_k\right)\left(\tilde{\boldsymbol{S}}_i\boldsymbol{b}_k\right)^H.\tag{23}$$

According to the definition $\tilde{\boldsymbol{S}}_i=\mathrm{E}\left[\boldsymbol{S}(t)\,x_i^*(t)\right]$, we derive

$$\begin{aligned}\tilde{\boldsymbol{S}}_i &= \mathrm{E}\left\{\mathrm{diag}\left[s_1(t),\ldots,s_P(t)\right]x_i^*(t)\right\}\\ &= \mathrm{diag}\left(\tilde{S}_{i,1},\ldots,\tilde{S}_{i,P}\right).\end{aligned}\tag{24}$$

where $\tilde{S}_{i,p}=\mathrm{E}\left[s_p(t)\,x_i^*(t)\right]$. Let $\boldsymbol{R'}_S=\tilde{\boldsymbol{s}}_i\tilde{\boldsymbol{s}}_i^H$ with $\tilde{\boldsymbol{s}}_i=\left[\tilde{S}_{i,1},\ldots,\tilde{S}_{i,P}\right]^T$. Inserting (24) into (23), we obtain

$$\begin{aligned}\sum_{k=0}^{M}\left(\tilde{\boldsymbol{S}}_i\boldsymbol{b}_k\right)\left(\tilde{\boldsymbol{S}}_i\boldsymbol{b}_k\right)^H &= \sum_{k=0}^{M}\mathrm{diag}(\boldsymbol{b}_k)\,\boldsymbol{R'}_S\,\mathrm{diag}(\boldsymbol{b}_k)^H\\ &= \sum_{k=0}^{M}\boldsymbol{D}^k\boldsymbol{R'}_S\left(\boldsymbol{D}^k\right)^H.\end{aligned}\tag{25}$$

Finally, $\sum_{i=-M}^{M}\tilde{\boldsymbol{S}}_i\tilde{\boldsymbol{A}}^H\tilde{A}\tilde{\boldsymbol{S}}_i^H$ in (15) can be written as

$$\sum_{i=-M}^{M}\tilde{\boldsymbol{S}}_i\tilde{\boldsymbol{A}}^H\tilde{\boldsymbol{A}}\tilde{\boldsymbol{S}}_i^H=\sum_{i=-M}^{M}\boldsymbol{X}_i=\sum_{k=0}^{M}\boldsymbol{D}^k\left(\sum_{i=-M}^{M}\boldsymbol{R'}_S\right)\left(\boldsymbol{D}^k\right)^H.\tag{26}$$

ACKNOWLEDGMENT

The authors would like to thank the anonymous reviewers and the Associate Editor for their valuable comments and

suggestions, which have greatly improved the quality of this paper.

REFERENCES

[1] L. C. Godara, "Application of antenna arrays to mobile communications. II. Beam-forming and direction-of-arrival considerations," *Proc. IEEE*, vol. 85, no. 8, pp. 1195–1245, Aug. 1997.

[2] H. Kim and M. Viberg, "Two decades of array signal processing research," *IEEE Signal Process. Mag.*, vol. 13, no. 4, pp. 67–94, Jul. 1996.

[3] J. Shi, G. Hu, X. Zhang, F. Sun, W. Zheng, and Y. Xiao, "Generalized co-prime MIMO radar for DOA estimation with enhanced degrees of freedom," *IEEE Sensors J.*, vol. 18, no. 3, pp. 1203–1212, Feb. 2018.

[4] W. Zhao, G. Li, C. Zheng, and F. Ge, "Capon cepstrum weighted l2, 1 minimization for wideband DOA estimation with sonar arrays," in *Proc. IEEE Oceans.*, Shanghai, China, Apr. 2016, pp. 1–4.

[5] R. Shafin, L. Liu, J. Zhang, and Y.-C. Wu, "DoA estimation and capacity analysis for 3-D millimeter wave massive-MIMO/FD-MIMO OFDM systems," *IEEE Trans. Wireless Commun.*, vol. 15, no. 10, pp. 6963–6978, Oct. 2016.

[6] L. Liu and H. Liu, "Joint estimation of DOA and TDOA of multiple reflections in mobile communications," *IEEE Access*, vol. 4, pp. 3815–3823, 2016.

[7] R. O. Schmidt, "Multiple emitter location and signal parameter estimation," *IEEE Trans. Antennas Propag.*, vol. 34, no. 3, pp. 276–280, Mar. 1986.

[8] F. G. Yan, M. Jin, S. Liu, and X. L. Qiao, "Real-valued MUSIC for efficient direction estimation with arbitrary array geometries," *IEEE Trans. Signal Process.*, vol. 62, no. 6, pp. 1548–1560, Mar. 2014.

[9] H. Chen *et al.*, "RARE-based localization for mixed near-field and far-field rectilinear sources," *Digit. Signal Process.*, vol. 85, pp. 54–61, Feb. 2019.

[10] Y. Wu, A. Leshem, J. R. Jensen, and G. Liao, "Joint pitch and DOA estimation using the ESPRIT method," *IEEE/ACM Trans. Audio, Speech, Language Process.*, vol. 23, no. 1, pp. 32–45, Jan. 2015.

[11] T.-J. Shan, M. Wax, and T. Kailath, "On spatial smoothing for direction-of-arrival estimation of coherent signals," *IEEE Trans. Acoust., Speech, Signal Process.*, vol. 33, no. 4, pp. 806–811, Apr. 1985.

[12] S. U. Pillai and B. H. Kwon, "Forward/backward spatial smoothing techniques for coherent signal identification," *IEEE Trans. Acoust., Speech Signal Process.*, vol. 37, no. 1, pp. 8–15, Jan. 1989.

[13] P. Stoica, B. Ottersten, M. Viberg, and R. L. Moses, "Maximum likelihood array processing for stochastic coherent sources," *IEEE Trans. Signal Process.*, vol. 44, no. 1, pp. 96–105, Jan. 1996.

[14] M. Viberg and B. Ottersten, "Sensor array processing based on subspace fitting," *IEEE Trans. Signal Process.*, vol. 39, no. 5, pp. 1110–1121, May 1991.

[15] I. Ziskind and M. Wax, "Maximum likelihood localization of multiple sources by alternating projection," *IEEE Trans. Acoust., Speech Signal Process.*, vol. 36, no. 10, pp. 1553–1560, Oct. 1988.

[16] Y.-H. Choi, "Maximum likelihood estimation for angles of arrival of coherent signals using a coherency profile," *IEEE Trans. Signal Process.*, vol. 48, no. 9, pp. 2679–2682, Sep. 2000.

[17] G. Shi-Wei and B. Zheng, "Data-based matrix decomposition technique for high-resolution array processing of coherent signals," *Electron. Lett.*, vol. 23, no. 12, pp. 643–645, Jun. 1987.

[18] F.-M. Han and X.-D. Zhang, "An ESPRIT-like algorithm for coherent DOA estimation," *IEEE Antennas Wireless Propag. Lett.*, vol. 4, no. 12, pp. 443–446, Dec. 2005.

[19] Y. H. Choi, "ESPRIT-based coherent source localization with forward and backward vectors," *IEEE Trans. Signal Process.*, vol. 58, no. 12, pp. 6416–6420, Dec. 2010.

[20] C. Qian, L. Huang, W. J. Zeng, and H. C. So, "Direction-of-arrival estimation for coherent signals without knowledge of source number," *IEEE Sensors J.*, vol. 14, no. 9, pp. 3267–3273, Sep. 2014.

[21] X. Xu, Z. Ye, Y. Zhang, and C. Chang, "A deflation approach to direction of arrival estimation for symmetric uniform linear array," *IEEE Antennas Wireless Propag. Lett.*, vol. 5, pp. 486–489, Dec. 2006.

[22] W. Kai, Z. Yongshun, and S. Dan, "Novel algorithm on DOA estimation for correlated sources under complex symmetric Toeplitz noise," *J. Syst. Eng. Electron.*, vol. 19, no. 5, pp. 902–906, Oct. 2008.

[23] Y. Zhang, Z. Ye, and C. Liu, "An efficient DOA estimation method in multipath environment," *Signal Process.*, vol. 90, no. 2, pp. 707–713, Feb. 2010.

[24] Y. Zhang, Z. Ye, X. Xu, and J. Cui, "Estimation of two-dimensional direction-of-arrival for uncorrelated and coherent signals with low complexity," *IET Radar Sonar Navigat.*, vol. 4, no. 4, pp. 507–519, Aug. 2010.

[25] B. Cai, Y.-M. Li, and H.-Y. Wang, "Forward/backward spatial reconstruction method for directions of arrival estimation of uncorrelated and coherent signals," *IET Microw., Antennas Propag.*, vol. 6, no. 13, pp. 1498–1505, Oct. 2012.

[26] C. Qi, Y. Wang, Y. Zhang, and Y. Han, "Spatial difference smoothing for DOA estimation of coherent signals," *IEEE Signal Process. Lett.*, vol. 12, no. 11, pp. 800–802, Nov. 2005.

[27] N. Yuen and B. Friedlander, "DOA estimation in multipath: An approach using fourth-order cumulants," *IEEE Trans. Signal Process.*, vol. 45, no. 5, pp. 1253–1263, May 1997.

[28] H. Chen, C.-P. Hou, Q. Wang, L. Huang, and W.-Q. Yan, "Cumulants-based Toeplitz matrices reconstruction method for 2-D coherent doa estimation," *IEEE Sensors J.*, vol. 14, no. 8, pp. 2824–2832, Aug. 2014.

[29] C. Qian, L. Huang, Y. Xiao, and H. C. So, "Localization of coherent signals without source number knowledge in unknown spatially correlated Gaussian noise," *Signal Process.*, vol. 111, no. 2, pp. 170–178, Jun. 2015.

[30] H. Shi *et al.*, "Efficient method of two-dimensional DOA estimation for coherent signals," *EURASIP J. Wireless Commun. Netw.*, vol. 2017, no. 53, pp. 1–10, Dec. 2017.

[31] F.-J. Chen, S. Kwong, and C.-W. Kok, "Esprit-like two-dimensional DOA estimation for coherent signals," *IEEE Trans. Aerosp. Electron. Syst.*, vol. 46, no. 3, pp. 1477–1484, Jul. 2010.

[32] S. Ren, X. Ma, S. Yan, and C. Hao, "2-D unitary ESPRIT-like direction-of-arrival (DOA) estimation for coherent signals with a uniform rectangular array," *Sensors*, vol. 13, no. 4, pp. 4272–4288, Apr. 2013.

[33] H. Chen and X. Zhang, "Two-dimensional DOA estimation of coherent sources for acoustic vector-sensor array using a single snapshot," *Wireless Pers. Commun.*, vol. 72, no. 1, pp. 1–13, Sep. 2013.

[34] C. Li, G. Liao, S. Zhu, and S. Wu, "An ESPRIT-like algorithm for coherent DOA estimation based on data matrix decomposition in MIMO radar," *Signal Process.*, vol. 91, no. 8, pp. 1803–1811, Aug. 2011.

[35] C. Chen and X. Zhang, "A coherent direction of arrival estimation method using a single pulse," *Comput. Electr. Eng.*, vol. 40, no. 5, pp. 1731–1740, Jul. 2014.

[36] S. Hong, X. Wan, F. Cheng, and H. Ke, "Covariance differencing-based matrix decomposition for coherent sources localisation in bi-static multiple-input–multiple-output radar," *IET Radar Sonar Navigat.*, vol. 9, no. 5, pp. 540–549, Feb. 2015.

[37] B. D. Rao and K. V. S. Hari, "Performance analysis of root-music," *IEEE Trans. Acoust., Speech, Signal Process.*, vol. 37, no. 12, pp. 1939–1949, Dec. 1989.

[38] P. Stoica and N. Arye, "MUSIC, maximum likelihood, and Cramer-Rao bound," *IEEE Trans. Acoust., Speech Signal Process.*, vol. 37, no. 5, pp. 720–741, May 1989.

WEI ZHANG was born in Yinchuan, China, in 1981. She received the B.S. degree in electronic and information technology and the M.S. degree in communication and information system from Lanzhou University, Lanzhou, China, in 2003 and 2006, respectively. She is currently pursuing the Ph.D. degree with the Harbin Institute of Technology, Harbin, China. Since 2006, she became a Lecturer with North Minzu University, Yinchuan. Her research interests include array signal processing and their applications.

YONG HAN was born in 1976. He received the Ph.D. degree from the Harbin Institute of Technology, Harbin, China, in 2010. He is currently a Lecturer with the School of Information and Electrical Engineering, Harbin Institute of Technology, Weihai, China. His research interests include array signal processing and polarization sensitive array signal processing.

MING JIN was born in Liaoning, China, in 1968. He received the B.E., M.S., and Ph.D. degrees in information and communication engineering from the Harbin Institute of Technology, China, in 1990, 1998, and 2004, respectively. From 1998 to 2004, he was with the Department of Electronics Information Engineering, Harbin Institute of Technology. Since 2006, he has been a Professor with The School of Information and Electricity Engineering, Harbin Institute of Technology, Weihai. His current interests include array signal processing, parallel signal processing, and radar polarimetry.

XIAOLIN QIAO was born in 1948. He received the B.E., M.S., and Ph.D. degrees in information and communication engineering from the Harbin Institute of Technology, Harbin, China, in 1976, 1983, and 1991, respectively. His research interests include signal processing, wireless communication, special radar, parallel signal processing, and radar polarimetry.